Materials and Structures, 1993, **26**, 414–424

Effect of fly ash on the microstructure of cement mortar

A. XU*, S. L. SARKAR‡, L. O. NILSSON*

*Division of Building Materials, Chalmers University of Technology, Göteborg, Sweden
‡Faculty of Applied Sciences, University of Sherbrooke, Sherbrooke, Québec, Canada J1K 2R1

A microstructural study of mortars prepared with a low-alkali, low-C_3A cement and a Class F fly ash, both of Swedish origin, was carried out using the scanning electron microscopy–energy-dispersive X-ray analytical technique. Supplementary phase analyses were made by X-ray diffraction and thermogravimetry–differential thermal analysis. Normally, CH crystals in the transition zone grow with their c axis parallel (or the (0 0 1) cleavage plane perpendicular) to the aggregate surface. The encapsulation of the fly ash particles by the growing CH reduces the amount of orientated CH at the aggregate–paste interface. The growth mechanism of these crystals is discussed. The reduction of CH, most significant after 28 days of hydration, is mainly due to the reaction of CH with the fly ash glass phase. Initially, the replacement of cement by fly ash weakens the paste–aggregate interfacial zone due to reduction of contact points, and increases the local water-to-cement ratio. This, however, improves significantly when the fly ash has reacted. In order to enhance the reaction of fly ash, extra gypsum was added. The results show that gypsum can accelerate the fly ash reaction, but the products formed, and the beneficial effects of gypsum, are mainly determined by the total amount of gypsum in the paste.

1. INTRODUCTION

The replacement of cement with fly ash, especially low-calcium fly ash (ASTM Class F), has been shown to have a significant effect on the properties of concrete; typically, it leads to a lower early strength with a potential for later-age strength gain [1]. It was recognized that the change in properties is closely related to the concrete's microstructure, which is affected by the fly ash both physically and chemically [2].

Several researchers have advanced a number of hypotheses to explain the microstructural effect of fly ash incorporation in concrete [3]. Kokubu's review article [4] concluded that the main effect of fly ash was the 'finely divided powder effect', i.e. the ash increases the available space in the floc structure created by cement particles, thus enhancing the cement hydration. This phenomenon has been pointed out by several researchers, including Gutteridge and Dalziel [5], who showed that, by replacing cement with fly ash (30 parts by weight), the degree of hydration of the C_3S and C_3A (at a water-to-solid ratio of 0.71) is enhanced after about 7 h. The enhancement reached its maximum after several hours, depending on the ash used. The enhancement effect also occurs when cement is blended with 5% TiO_2 (rutile) [6]. Takemoto and Uchikawa [2], who summarized several pozzolanic reaction mechanisms, emphasized that fly ash preferably adsorbs Ca^{2+} and provides the precipitation sites for cement hydration products such as ettringite (AFt) and calcium hydroxide (CH), so that the C_3A hydration is accelerated. Under OH^- attack, the fly ash glass phase dissolves and reacts to form plate-like or fibrous C–S–H phases that interlink the particles.

Diamond [7] pointed out that in the fly ash–cement paste, the fly ash particles are often covered with a layer of fibrous hydrates termed 'duplex film', because of its similarity to that which develops on the aggregate surface of concrete. Diamond explained this as deposition of cement hydration products like CH and C–S–H (I) phase. The phenomenon was further elucidated by Montgomery *et al.* [3] as fly ash acting as the nucleation centres for cement hydration.

Cabrera and Plowman [8], on the other hand, demonstrated that hydration products in the flaky form appear on the fly ash surface as early as 3 days, indicating prompt fly ash hydration. That hydration is more rapid at higher temperatures, evident from surface erosion as shown by Montgomery *et al.* [3], whereas Huang [9] claims that the reaction can be further accelerated by the addition of extra gypsum.

However, fly ash hydration and concrete strength development are not always well correlated. Cabrera and Plowman [8] observed surface erosion of fly ash at about three weeks of curing without any corresponding strength increase in the concrete. According to Diamond [10], the fly ash reaction differs from particle to particle. In general, low-calcium fly ash has limited reaction properties, and some particles retain a smooth surface even at 1 year. Thus, Diamond questions the idea that pozzolanic reaction of fly ash leads to extra strength gain in concrete after about a month. Hydrated or not, the fly ash particles are readily distinguishable from the surrounding paste under the scanning electron microscope. This gives a unique opportunity to study its microstructure and correlate its hydration reaction with the strength development pattern.

In the present investigation the microstructure of cement–fly ash mortar in relation to the strength development and hydration was studied with special attention paid to the morphology and composition of the hydration products of fly ash in the cement paste, comparison of the bulk paste structure with that of the paste–aggregate interfacial zone, and the effect of additional gypsum on the strength and microstructure.

2. EXPERIMENTAL PROCEDURE

2.1 Materials

A low alkali, low C_3A cement (Cementa AB, Sweden) was deliberately chosen to amplify the fly ash reaction which may result in the formation of calcium aluminate hydrate phases [11]. A fly ash relatively rich in alkali derived from the combustion of bituminous coal (provided by the Västerås City Thermopower Plant, Sweden) was selected. The chemical composition of the cement and fly ash is shown in Table 1.

A nearly pure quartz sand 0.5–1.5 mm in size was used for the mortar mix. The mix proportions were binder:water:sand = 1.00:0.46:2.50. 40 mm × 40 mm × 160 mm mortar prisms, prepared for flexural and compressive strength testing, were cured in water at room temperature (20°C) till the scheduled time, i.e. 1, 3, 7 or 28 days (and 180 days for compressive strength). The fly ash content was varied at fly ash/(cement + fly ash) = 0, 0.30 and 0.60. In addition, two mixes containing additional gypsum ($CaSO_4 \cdot 2H_2O$) at a gypsum/fly ash ratio of 0.10 were also cast to study the effect of gypsum addition on the strength and microstructure of fly ash–cement mortar.

2.2 Sample preparation

Pastes of the same mix proportions as the mortar were prepared (shaking until setting occurred to prevent sedimentation) and cured in water in sealed containers. These were used to study the hydration process. The samples were dried at the scheduled ages by immersing them in pure acetone for 30 min, followed by drying at 60°C to constant weight.

2.3 Strength determination

The flexural strength was determined according to ASTM C 348 and compressive strength according to ASTM C 349 (using portions of prisms broken in flexural testing). The results reported are the averages of three specimens for flexural and six for compressive strengths, respectively.

2.4 Evaluation of the hydration process

Thermogravimetry and differential thermal analysis (TG–DTA) and X-ray diffraction (XRD) analysis were performed to determine the content and composition of the unhydrated cement component and hydration products in order to evaluate the progress of hydration. The paste samples for XRD were finely ground to eliminate preferred orientation.

TG and DTA were carried out using a Seiko SII SSC/5200 TG/DTA. The mass of the sample used ranged from 30 to 50 mg, with a fine α-Al_2O_3 powder of similar weight as the reference material. The temperature increment was 10°C min^{-1} from 25 to 1100°C in an N_2 atmosphere (100 ml min^{-1}).

XRD analysis was performed on a Rigaku D-Max X-ray diffractometer (CuK_α radiation, 40 kV, 35 mA), in a scanning range of 5 to 60° in 2θ at an interval of 0.001°. Semi-quantitative analysis was done by integrating the intensity of the peaks of interest.

A Jeol JSM-840A SEM equipped with a Link 100085 for energy-dispersive X-ray analysis (EDXA) was used for the microstructural examination and quantitative elemental analysis of phases.

3. RESULTS

3.1 Strength

The compressive (up to 180 days) and flexural strength (up to 28 days) of the mortars at different ages illustrated in Fig. 1 clearly show that the compressive strength decreases with an increase in the amount of fly ash. The trend is similar for the flexural strength. It appears that the decrease in flexural strength due to high-volume fly ash replacement is less than that in the compressive strength. Comparing the mortars containing cement and fly ash with their counterparts containing additional gypsum, one can see that the strength of mortars with gypsum is lower at an early age (before 7 days), but significantly higher at 28 days.

The long-term (180 days) compressive strength is slightly higher (59 MPa) for the mortar with 30% fly ash than that of the plain cement mortar (56 MPa). The strength of the 60% fly ash mortar also reaches nearly

Table 1 Chemical composition of cement and fly ash

Material	CaO	SiO_2	Al_2O_3	Fe_2O_3	MgO	SO_3	K_2O	Na_2O
Cement[a]	64.2	22.3	3.46	4.82	0.84	2.06	0.69	0.03
Fly ash[b]	7.2	47.3	22.8	9.31	4.00	1.00	2.60[c]	

[a] $C_3A < 1\%$.
[b] Ignition loss 3.50%.
[c] Total alkalis as Na_2O.

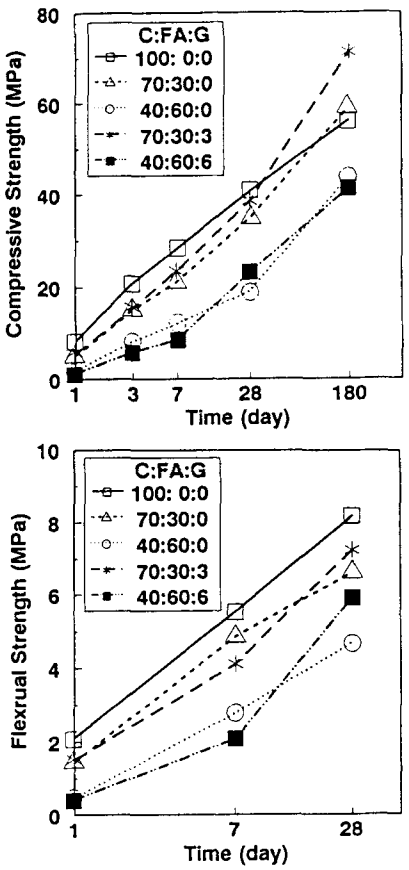

Fig. 1 Strength development of mortar samples.

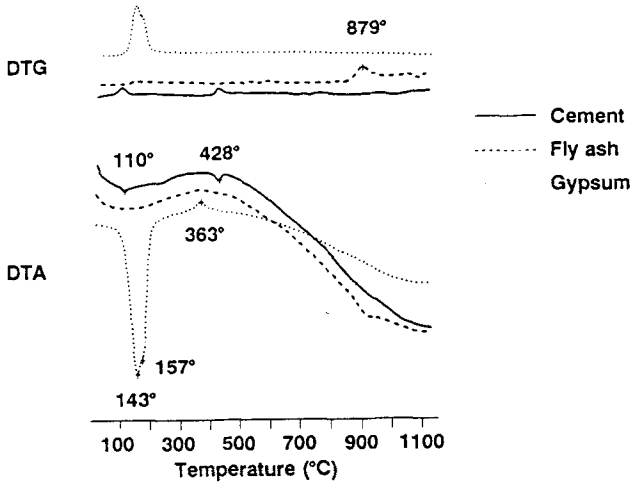

Fig. 2 DTG–DTA of as-received cement, fly ash and gypsum.

80% of that of the plain cement mortar. It is evident that addition of gypsum to the fly ash–cement mortar accelerates the strength development process, and in the case of the mortar with 30% fly ash and additional gypsum this is much more pronounced. However, the strength is slightly lower for the mortar with 60% fly ash and gypsum compared with its counterpart with no additional gypsum.

3.2 TG–DTA

TG results rearranged into (differential thermogravimetry (DTG)) curves are shown in Figs 2 and 3. In Fig. 2 the as-received cement develops weak endothermic peaks at about 115 and 430°C, which can be due to a mild hydration of the cement in the presence of air moisture. The fly ash exhibits a distinct weight loss starting at about 500°C, which suddenly becomes more rapid at 850°C and continues to higher temperatures. This is partly attributable to the volatile matter in the unburnt coal [12]. Gypsum shows strong endothermic peaks at 144 and 157°C due to the dehydration of $CaSO_4.2H_2O$ to β-$CaSO_4.\frac{1}{2}H_2O$ and then to β-$CaSO_4$. A weak exothermic peak at 363°C is due to the lattice change of $CaSO_4$ [13].

In Fig. 3, the hydrated cement has a characteristic endothermic peak at 460°C due to decomposition of CH [14] which shifts to a higher temperature with hydration time, from 436°C at 2 h to 478°C at 28 days. The 127°C endothermic peak at 2 h could be due to the presence of a small amount of gypsum in the cement, though this is about 20°C lower than for pure gypsum, confirmed from the samples with additional gypsum. The broad endothermic peak at temperatures up to 400°C is due to the decomposition of calcium silicate hydrate (C–S–H) (ca. 150°C) [14], ettringite (ca. 140°C), and calcium aluminate hydrates (200–300°C) [15]. Though the samples containing fly ash have similar DTA curves, the CH peak occurs at a lower temperature together with a distinct endothermic peak at about 170°C due to the formation of monosulphate hydrate [15]. In the samples with additional gypsum, especially in the 60% fly ash paste, more ettringite is formed at 90 days.

At temperatures of 600–700°C, an obvious weight loss accompanied by an endothermic effect occurs for all the samples, which may be due to slight carbonation during drying and grinding. The samples containing fly ash additionally show a significant weight loss corresponding to an endothermic effect at 750–900°C. For the samples with additional gypsum, this effect extends to about 1000°C.

Fig. 4 shows the weight loss on heating samples to 400°C. This is due to the release of non-evaporable water (Wn) by different water-bearing compounds (except CH), which is an approximate measure of the degree of hydration. Since the pozzolanic reaction consumes CH, its content in the paste containing fly ash cannot be used to express the amount of hydration products at later ages. The pastes with fly ash are seen to have a higher Wn content than that produced by the cement. A stronger effect is observed in the pastes containing additional gypsum.

3.3 XRD analysis

The XRD patterns (Fig. 5) not only confirm the TG–DTA results, but also provide additional information about the mineral phases. Strätling's compound (C_2ASH_8), aluminate hydrates, C_2AH_{8-13}, C_4AH_{13}, and other

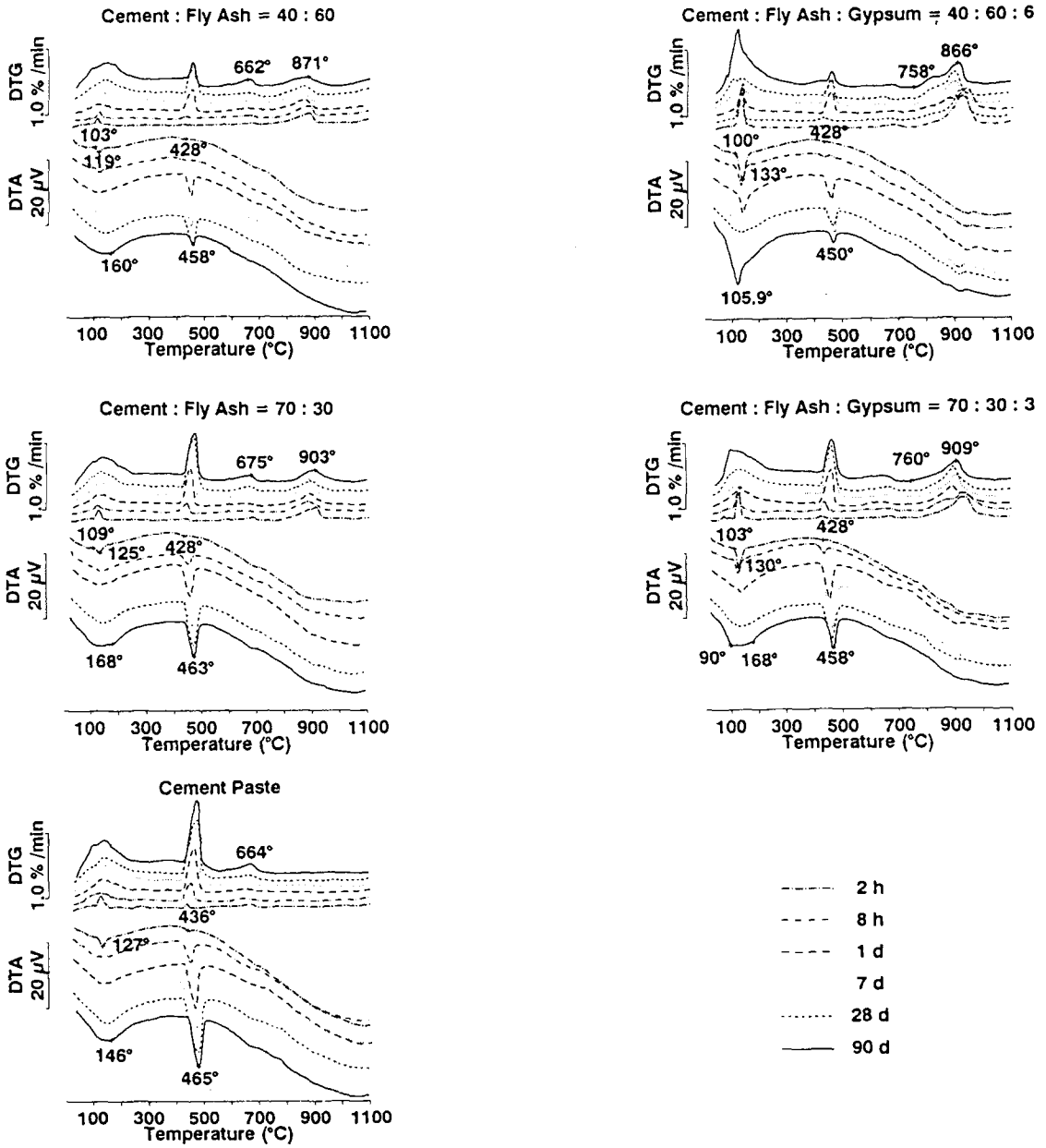

Fig. 3 DTA and DTG analyses of pastes at different ages.

hydration products such as C–S–H (II) and $C_{1.5}S_{3.5}H_x$ form in the fly ash pastes, whereas, at 90 days, greater amounts of ettringite form in the pastes with additional gypsum. Some other hydrated phases, such as $Al_2(SO_4)_3 \cdot H_2SO_4 \cdot 8H_2O$, were also identified in the high fly ash, high gypsum paste. Interestingly enough, even at 90 days, a large fraction of cement C_4AF phase remains unhydrated.

Since peak intensity analysis of different C_3S peaks shows a very similar trend, only the (6 2 0) C_3S peak (ca. 51° 2θ) intensities are plotted in Fig. 6. The content of unhydrated cement in the pastes at different ages is nearly proportional to their original cement content. Fig. 7a shows the integrated intensity of the (1 0 1) CH peak as a function of hydration age. At a very early age, i.e. at 2 h, the relative amount of CH is higher than the fraction of cement in the mixes containing fly ash, but later

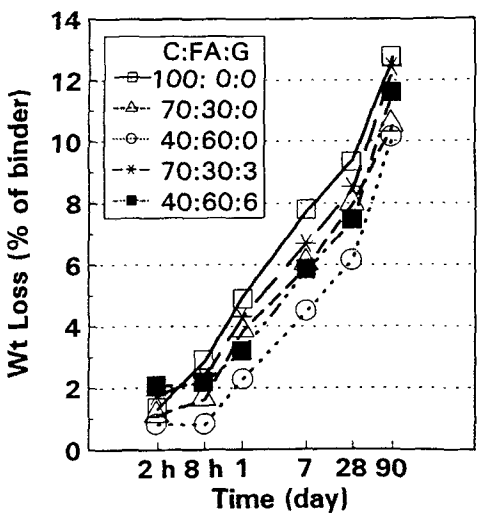

Fig. 4 Weight loss of pastes heated to 400°C.

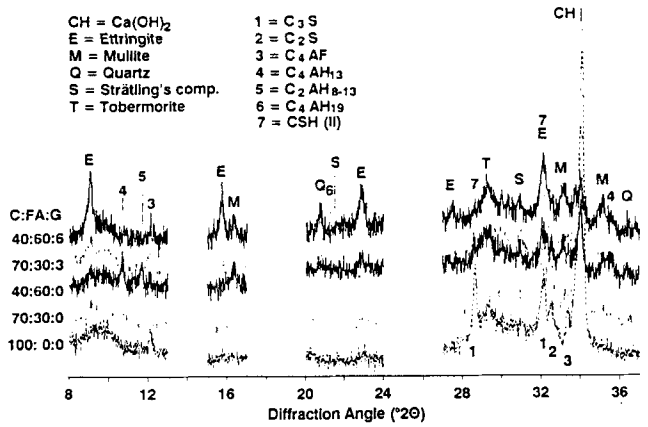

Fig. 5 XRD patterns of pastes at 90 days.

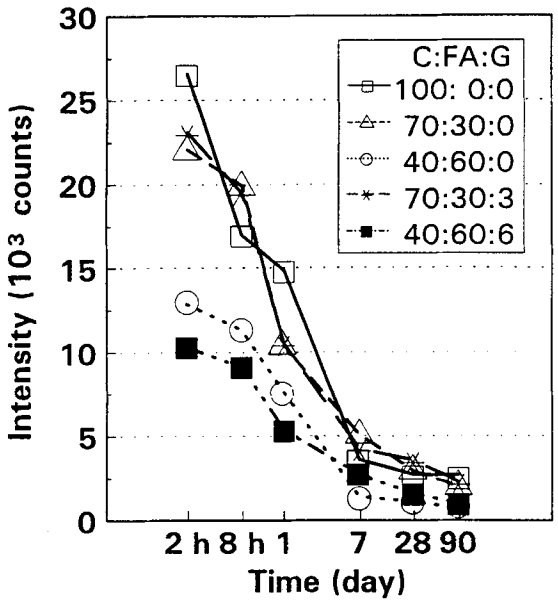

Fig. 6 Integrated XRD intensity of C_3S (6 2 0) peak at different ages.

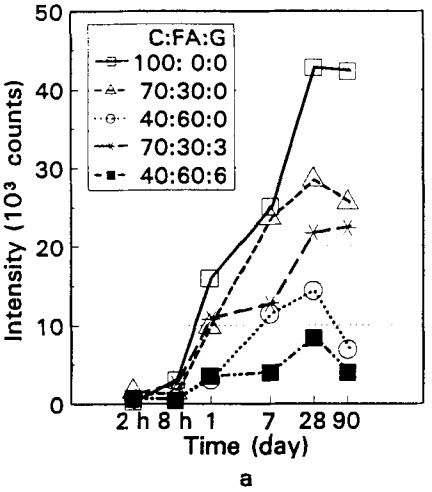

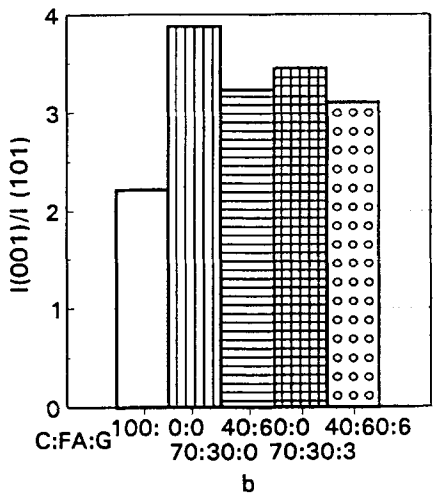

Fig. 7 (a) Integrated intensity of (1 0 1) CH peak at different ages; (b) $I_{(001)}/I_{(101)}$ at 28 days.

decreases substantially for the mix with fly ash and with the additional gypsum. The CH content for all the mixes at 90 days is the lowest, indicating consumption of CH.

The ratios $I_{(001)}/I_{(101)}$ at 28 days are shown in Fig. 7b. $I_{(001)}/I_{(101)} = 0.74$ for portlandite in the JCPDS file. Hence, ratios higher than 0.74 are considered to be due to preferred orientation [16]. In this work this ratio was always higher than 2, and was 3.8 for the pastes with 30% fly ash.

3.4 SEM and EDXA

The fly ash used in this study is generally smooth and spherical, and mainly consists of elements such as Al, Si, K, as seen in Fig. 8. The particle size of the fly ash ranges from 1 μm to about 100 μm, with an average of 20 μm. From EDXA, the Ca:Si:Al:K ratios determined were 0.25:54.5:39.9:5.3.

Some fly ash particles are relatively rich in Fe at the expense of Si and Al. The surface of these particles is usually rough, and probably readily adsorbs Ca ion at an early hydration age, which gives it the appearance of being highly reacted.

The microstructural development of fly ash pastes has been described elsewhere by two of the present authors [11]. The mortar microstructure is similar to that of the paste, except for the region around the aggregate. In the mortar without fly ash, typically but not always, CH crystallizes with the *c* axis parallel (or the cleavage plane perpendicular) to the aggregate surface and grows directly on the aggregate with a terraced structure (Fig. 9). Occasionally, C–S–H gel is formed on the CH which changes the crystalline direction of the latter. In the absence of CH growth, a layer of C–S–H gel is formed. A gap of 0.5 to 1 μm between CH crystals, parallel to the cleavage plane, was often observed. Microcracks (possibly formed during fracturing of the sample) exist between the boundaries of the crystalline phases.

Replacement of cement with fly ash reduces the amount of CH in the paste. However, XRD analysis confirms that the preferred orientation of CH is little influenced by fly ash. Fig. 10 shows that CH crystallizes with its cleavage plane perpendicular to the aggregate surface,

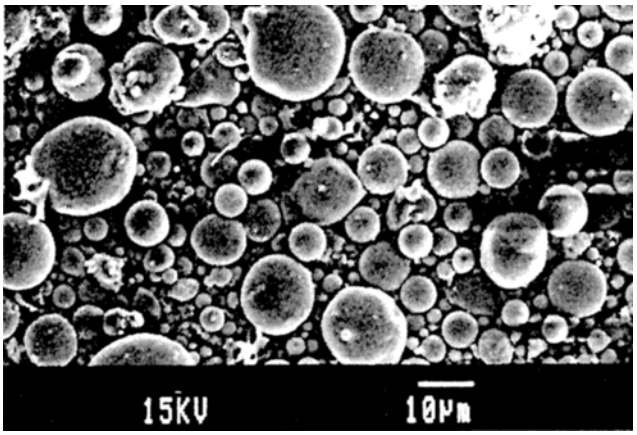

(a)

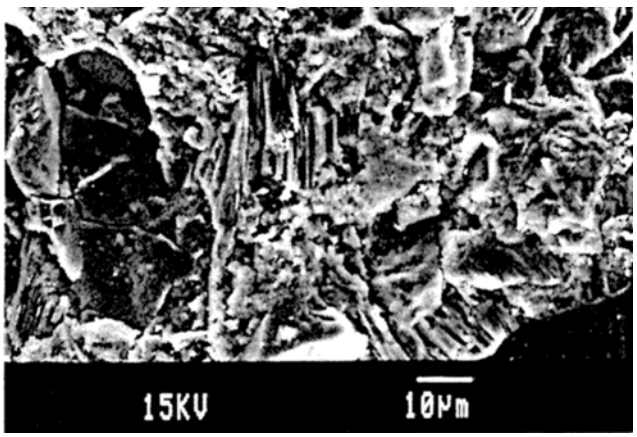

(b)

Fig. 8 (a) Fly ash particles and (b) their elemental analysis.

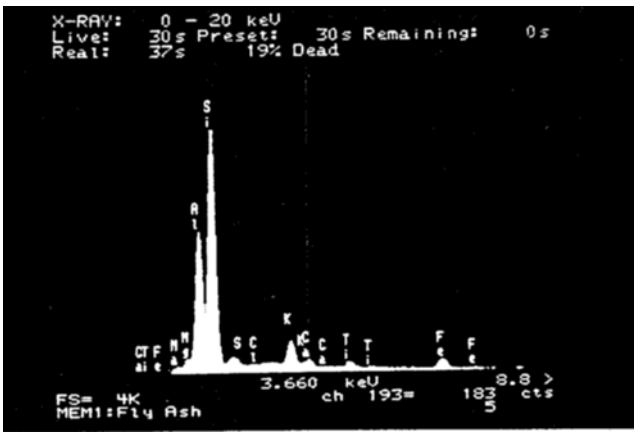

(a)

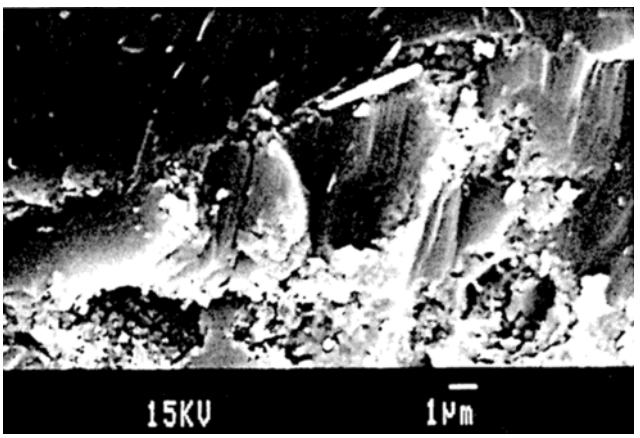

(b)

Fig. 9 CH formed in the mortar without fly ash: (a) general view, (b) CH with the cleavage plane perpendicular to the surface of an aggregate.

but this feature is absent at the interface where fly ash particles appear to hydrate. The structure of the interfacial zone, which extends to about 10 µm thick, can be rather porous (Fig. 11).

As shown in Fig. 1, the mortar with 30% fly ash and additional gypsum has a much higher long-term strength than all the others. Correspondingly, the hydration products are seen to be much more homogeneously distributed in this mortar (Fig. 12), making its microstructure dense. However, there still exist well-crystallized CH crystals that surround fly ash particles and are inclined to the aggregate surface. The surface of fly ash particles encapsulated by the CH is generally heavily eroded (Fig. 13).

A homogeneous interfacial zone was also encountered in the mortar with 60% fly ash and additional gypsum. Around fly ash particles, a 1 to 2 µm thick layer of hydration products grows radially outward, but a less dense interfacial paste zone develops at the aggregate surface. No distinguishable duplex film was visible in the vicinity of the aggregate (Fig. 14). Unlike its paste counterpart, the mortar contains almost no ettringite crystals in the paste *per se*, though large ettringite needles were detected in the entrapped air voids (Fig. 15). The

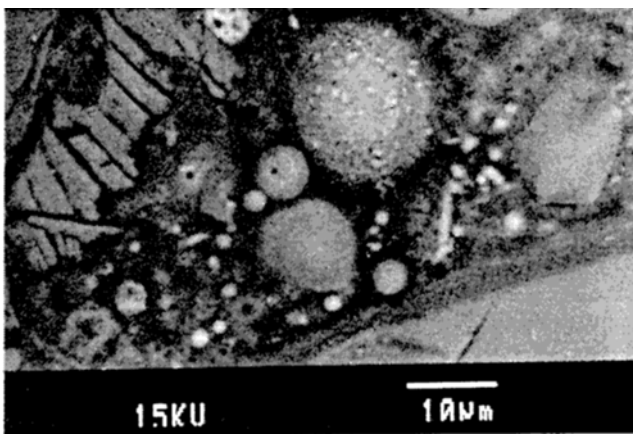

Fig. 10 Back-scattered image of mortar with 60% fly ash at 90 days.

fly ash particles are homogeneously distributed in the paste between the aggregates, and several are in direct contact with the aggregate (Fig. 16). A thin layer of dark zone around fly ash particles appears in the back-scattered

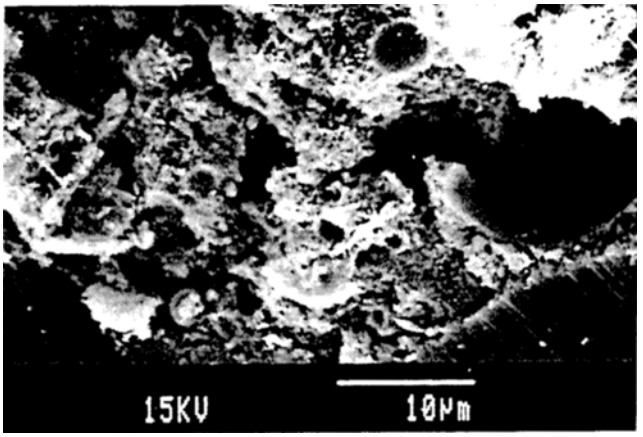

Fig. 11 Porous interfacial zone. Mortar with 60% fly ash, at 90 days.

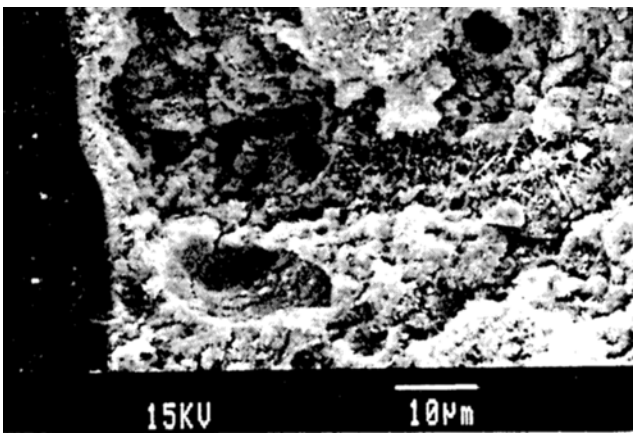

Fig. 12 Hydration products near aggregate. Mortar with 30% fly ash and additional gypsum at 90 days.

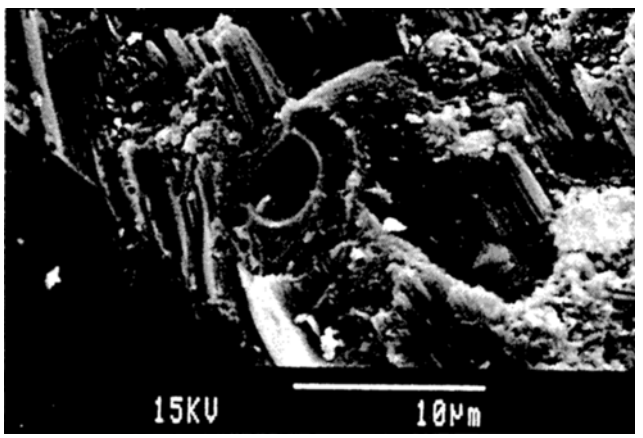

Fig. 13 The interfacial zone in cement–30% fly ash–gypsum mortar.

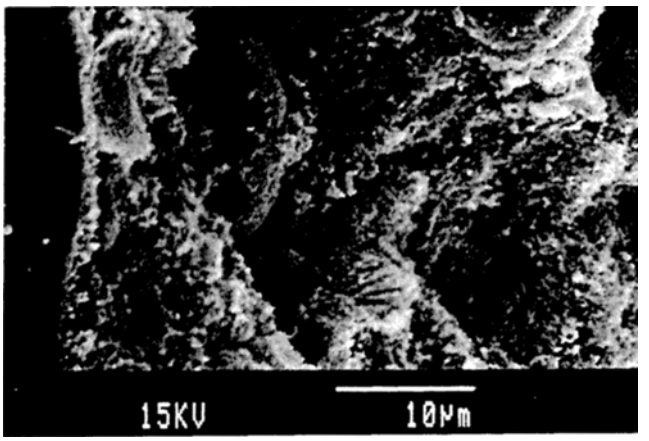

Fig. 14 The paste–aggregate interface in cement–60% fly ash–gypsum mortar.

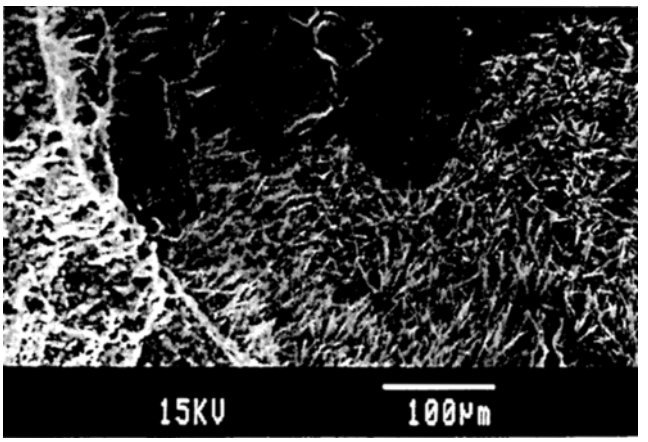

Fig. 15 Ettringite needles in voids.

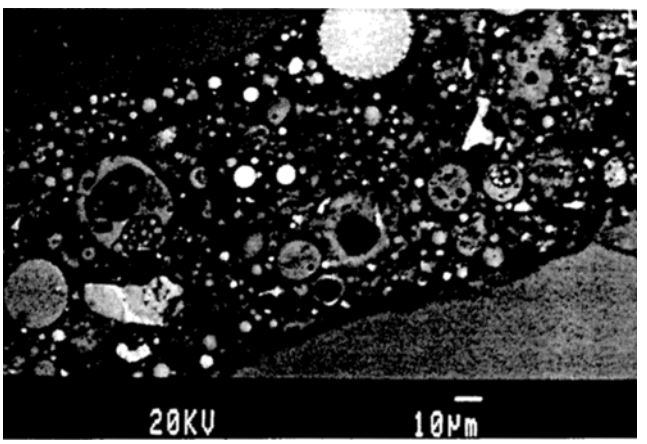

Fig. 16 Homogeneous distribution of fly ash particles in the paste of cement–60% fly ash–gypsum mortar.

image, which indicates that its density is low and can be attributed to the hydrated phase and to pores.

Elemental mapping (Fig. 17) confirms that the layer of reacted fly ash is very thin, and shows that S and Ca diffuse into the hollow core of the fly ash through some weak points in the wall [11]. The distribution of Ca is rather definite, whereas those of S and K are more diffuse.

Along with the SEM examination, the composition of the cement, fly ash and hydration products was qualitatively analysed by EDXA. The hydrated phases, composed of Ca, Si, Al, and other minor elements in

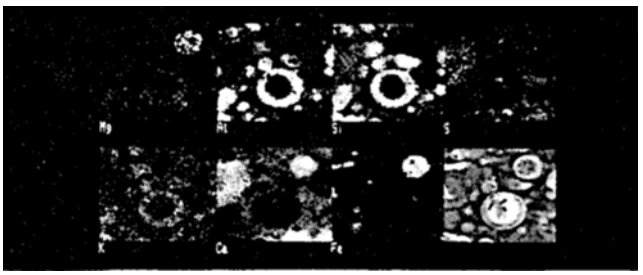

Fig. 17 Elemental map of fly ash particles and the surrounding paste. Paste with 60% fly ash and additional gypsum.

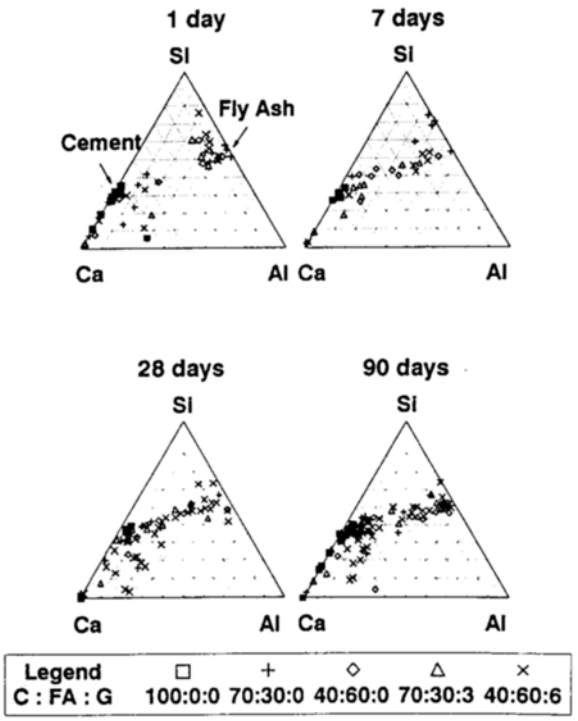

Fig. 18 Ternary diagram of the main elements in the cement–fly ash pastes, based on EDXA results. Atoms of Ca + Si + Al + K = 100%. C = cement, FA = fly ash, G = gypsum.

varying proportions, are illustrated in Fig. 18. The K content varies in the range of 0 to 6%, being higher in the samples with fly ash without the additional gypsum at early ages, before 7 days. With hydration, the Ca/Si ratio of the cement hydrates decreases from an average of 2.3 at 1 day to 1.7 at 90 days. This ratio, though high at 1 day for the hydration product on or near the fly ash, is lower than 1.7 at 90 days. The concentration of K on the fly ash surface decreases with time, but most of it remains inside the fly ash particles as shown in Fig. 17.

4. DISCUSSION

The hydration products of cement around aggregates, though essentially the same as those in the bulk paste, develop different morphological features. Fly ash influences the microstructure of both the bulk paste and the aggregate–paste interfacial zone.

In plain cement mortar, orientated CH crystals grow on the aggregate surface, often with the (0 0 1) plane perpendicular to the aggregate surface. The present SEM observations are in agreement with those of other researchers such as Larbi and Bijen [17,18], but are inconsistent with the conclusion, drawn on the basis of XRD studies, that CH grows with its *c*-axis perpendicular to the aggregate [19,20].

This growth phenomenon can be explained by the crystal growth theory [22] which states that a crystal grows faster at right-angles to the face on which the atoms deposit, and the best-developed faces of the final crystal are those which build up most slowly. The latter process eliminates a face along the *a* or *b* axis; thus CH in the paste rarely shows a hexagonal shape. The growth of CH along the *c*-axis direction may be due to face defects such as terraces, steps, or screws.

At the C–S–H-deposited areas on the aggregate surface, the general growth direction may not be at right-angles to the aggregate surface. Larbi and Bijen [18] explained this as due to impurities adsorbed on the aggregate surface serving as the nuclei for CH growth. On the other hand, crystal growth may be arrested by the adsorption of impurities in the defect zone. Therefore, spaces containing C–S–H gel are often seen (Fig. 9).

In this light, the CH-encapsulating fly ash particles can be partly explained by the nucleation of CH on them, in view of the alkali released from fly ash which leads to a locally high pH condition. The high solubility of alkaline salts causes a 'common ion effect' which reduces the CH solubility. Thus, CH tends to precipitate out earlier. Nevertheless, the unidirectional growth of tabular CH crystals around fly ash particles instead of radial growth needs further explanation. It can be assumed that smaller crystals have a higher solubility, so that they redissolve and recrystallize on the larger crystals [22]. Another possibility is that Ca^{2+} supplied by the cement hydrates diffuses gradually towards the fly ash particles on which the CH crystallizes, thus encouraging the CH to grow mainly towards the cement grain. Hence, when fly ash particles are very close to the aggregate, the crystalline direction of CH growth on aggregate is no longer perpendicular to the aggregate as shown in Fig. 13.

One must, however, note that C–S–H gel-like hydration products surrounding fly ash particles were more frequently observed than CH. At very early ages, a layer of fibrous hydration products forms on fly ash particles which grows to a length of about 1 μm, and whose morphology is similar to that of the hydration products in plain cement paste. Apparently, this is formed by the deposition of cement hydration products [10]. However, EDXA shows that the hydration products near the fly ash contain more Al than those near the cement grains, indicating dissolution and reaction of Al from fly ash particles. This assumption is also supported by the XRD analysis, which shows that the hydration of the aluminate-bearing phase C_4AF in the cement (the cement being very low in C_3A) is quite slow (Fig. 5). Besides, different calcium aluminate hydrates, AFm and AFt

phases and Strätling's compound, are only found in the pastes with fly ash. Moreover, the obvious reduction in CH after 1 day in the pastes with fly ash also indicates the reaction of fly ash.

The average Ca/Si molar ratio of 1.7 of the hydration products of the cement is in agreement with a previous researcher's results [23]. The Ca/Si ratio is lower for the fly ash hydrates, though it increases with hydration time. The low Ca/Si ratio C–S–H, as mentioned by Taylor [23], can be tobermorite (e.g. 11 nm tobermorite $C_5S_6H_5$). The XRD patterns show $C_{1.5}S_2H_x$ in the late-age pastes. According to Taylor the Ca/Si ratio increases with a decrease in the silicate tetrahedra chain length. Thus, the products of fly ash reaction contain long-chain silicate tetrahedra.

The enhanced hydration due to the finely divided powder effect exerted by fly ash [4] is not obvious from either XRD analysis of the unhydrated cement or the non-evaporable water from DTG. This may be due to the combined effect of fly ash on the cement–water system and the pore system. Firstly, replacing cement by fly ash dilutes the cement concentration. Secondly, the addition of fly ash increases the water-to-cement ratio W/C:

$$\frac{W}{C} = \frac{W}{C+F}\left(1 - \frac{F}{C+F}\right)^{-1} \quad (1)$$

where W, C and F denotes unit weight of water, cement and fly ash. Thirdly, it decreases the total initial porosity, given by

$$\frac{V_W}{V_W + V_C + V_F + V_S} = \frac{W}{C+F}\left[\frac{W}{C+F} + \frac{1}{\rho_C} + \frac{F}{C+F}\left(\frac{1}{\rho_F} - \frac{1}{\rho_C}\right) + \left(\frac{S}{C+F}\right)\frac{1}{\rho_S}\right]^{-1} \quad (2)$$

where V denotes volume, ρ specific gravity, S the unit weight of sand, and subscripts C, F and S denote cement, fly ash and sand, respectively. Another important factor is that the dissolution of fly ash releases silicate and aluminate ions into solution. In addition to this, the fine particles themselves provide nucleation centres for hydration products.

In brief, dilution of cement reduces the heat released during cement hydration at early age, which, in turn, reduces the hydration rate [24]. The increase in water-to-cement ratio reduces the degree of ion supersaturation in hydration products as stated by Kondo and Ueda [25]. On the other hand, Larbi and Bijen [26] suggest that the higher water content facilitates transport of Ca^{2+} to favourable nucleation sites for crystal growth. Whether this holds for the cement–fly ash mortar is debatable, as the total initial porosity is lower. The release of silicate and aluminate ions from fly ash, when it starts to hydrate, increases the concentration of these ions in solution. This lowers the silicate and aluminate ion gradient at the boundary between cement grain and water. Thus the cement hydration at a later age may be hindered. However, the total amount of hydration products is still high due to the formation of products with a lower Si/Ca in this system.

In addition to cement dilution and the fact that the fly ash reaction is essentially a 'secondary reaction' that depends on cement hydration, the lower early-age strength of the fly ash mortars may be due to poor contact between (a) fly ash and cement paste, (b) fly ash particles, and (c) fly ash and aggregate, the last being highly significant, because the mixing water adsorbed on the fly ash and aggregate surfaces builds up a locally higher water-to-cement ratio. This increases the local porosity due to a wall effect on the compact density [27]. Obviously, the porous nature of these zones affects the mortar strength. It also facilitates the crystallization and growth of CH. This is also considered as the major flaw in concrete; CH exhibits low strength between cleavage planes (only about 1 MPa) [19]. The fly ash at a late age thus has a twofold effect, i.e. it strengthens the contact between particles and also consumes CH to reduce this flaw. As shown in Fig. 1, the low-volume fly ash mortar strength surpasses that of plain cement mortar at 180 days. Nevertheless, the reaction of fly ash is a particle-to-particle phenomenon, which occurs earlier in some particles and later in others. Thus, one must not expect a sudden strength increase when reaction symptoms appear only on some particles, as was described by previous researchers [8].

The strength enhancement of additional gypsum was previously discussed [11]. While it is true that in the low-volume fly ash–gypsum mortar the strength increases continuously, and is higher than that of plain cement mortar at 180 days, the effect is not so obvious in the high-volume fly ash content mortar. It is suspected that this is because the actual cement content in this mortar is very low. Besides, the detrimental effect of excessive ettringite in the paste might be another reason, though no evidence of this came to light from microstructural observations.

The gypsum–fly ash pastes were seen to have a large weight loss at 900°C in TG–DTA. Though the starting temperature becomes lower for the older pastes (Fig. 3), the total amount does not change much with age. The weight loss at this particular temperature is usually attributed to the decomposition of $CaCO_3$ [13]. The presence of carboaluminate hydrates such as $C_3A.yCaO.(1\text{-}y)CaCO_3.H_x$, $C_3A.CaCO_3.H_x$, and $C_3A.3CaCO_3.H_{32}$ [15] may also contribute to this. The authors tested the possibility of carbonation by immersing the samples in hydrochloric acid, but found no evidence to support the idea that more CO_2 is released from the fly ash–gypsum pastes. On the other hand, the weight loss at 600–700°C, which occurs for all the samples, may account for the decomposition of $CaCO_3$. This low temperature (compared with the 890°C decomposition temperature for pure crystalline calcite) indicates the poor crystallinity of the calcium carbonate in these pastes. Moreover, the presence of carbonate-bearing compounds is not obvious from the XRD patterns. Ahmed *et al.* [28] showed that the weight loss of a sample

containing C_4AH_{12} at 740–880°C (dynamic) corresponds to the loss of the remaining hydroxyl ions. It is possible that fly ash hydrates, due to their high aluminate-phase contents, retain some bound OH^- that can be released only at high temperature. The remarkable weight loss difference between the samples with and without gypsum at 900°C is obviously related to the gypsum. The SO_4 from gypsum can combine with the fly ash glass phase, whose decomposition occurs at this temperature. The reactions $Al_2(SO_4)_3 \rightarrow Al_2O_3 + 3SO_3$ and $SO_3 \rightarrow SO_2 + \frac{1}{2}O_2$ are known to occur between 700 and 900°C [12]. The decrease in the initial decomposition temperature indicates depolymerization of the glass phase, though this assumption needs further verification.

5. CONCLUSIONS

It is shown that fly ash has both enhancement and retardation effects on cement hydration. It also directly influences the pore system. The equal weight replacement of cement by fly ash lowers the total initial volumetric porosity of the mortar and increases the neat water-to-cement ratio. Fly ash may also provide nucleation centres for the growth of hydration products such as CH.

The preferred orientation of CH, however, is not reduced by the replacement of cement with fly ash. SEM observation of mortars shows that CH crystallized at the aggregate interface has cleavage planes either normal to or at an angle to the aggregate surface. In the case of fly ash mortar, the fly ash is often encapsulated by it.

With the progress of cement hydration, fly ash particles react chemically with Ca^{2+}, OH^- and SO_4^{2-} to form additional hydration products. Calcium silicate hydrates, calcium aluminate hydrates and calcium alumino-sulphate hydrates were positively identified. Nevertheless, the results show that the cement hydration is not distinctly accelerated in the presence of fly ash, though addition of an appropriate amount of gypsum to the fly ash mixes increases the hydration rate, and enhances the strength due to the build-up of a well-bonded microstructure. In addition, the consumption of CH by fly ash results in the reduction of CH at the aggregate–paste interface as well as in the bulk paste. This in turn decreases the flaws in the mortar and makes the matrix more homogeneous.

The higher weight loss for the fly ash mixes containing additional gypsum at 900°C remains unanswered. It is being suggested that this weight loss may be due to the decomposition of $CaSO_4$ whose decomposition temperature is lowered due to its reaction with fly ash.

REFERENCES

1. Berry E. E. and Malhotra, V. M., 'Fly Ash in Concrete', CANMET, Ottawa, SP85-3 (1986).
2. Takemoto, K. and Uchikawa, H., 'Hydration of pozzolanic cement', in Proceedings of 7th International Congress on the Chemistry of Cement, Paris, 1980, Vol. I (Editions Septima, Paris) pp. IV-2–1-29.
3. Montgomery, D. G., Hughes, D. C. and Williams, R. I. T.,y 'Fly ash in concrete – a microstructure study', *Cem. Concr. Res.* **11** (1981) 591–603.
4. Kokubu, M., 'Fly ash and fly ash cement', in Proceedings of 5th International Congress on Chemistry of Cement, Tokyo, 1968, Vol. IV (Cement Association of Japan, Tokyo) pp. 75–113.
5. Gutteridge, W. A. and Dalziel, J. A., 'Filler cement: the effect of secondary component on the hydration of Portland cement, Part 2. Fine hydraulic binders', *Cem. Concr. Res.* **20** (1990) 853–861.
6. *Idem.*, 'Filler cement: The effect of secondary component on the hydration of Portland cement, Part 1. A fine non-hydraulic filler', *ibid.* **20** (1990) 778–782.
7. Diamond, S., 'The characterization of fly ashes', in 'Effects of Fly Ash Incorporation in Cement and Concrete', Materials Research Society Symposium N, Boston, 1981, pp. 12–23.
8. Cabrera, L. G. and Plowman, C., 'The influence of pulverized fuel ash on the early and long term strength of concrete', in Proceedings of 7th International Congress on the Chemistry of Cement, Paris, 1980, Vol. III (Editions Septima, Paris) pp. IV 84–92.
9. Huang, S., 'Hydration of Fly Ash Cement and Microstructure of Fly Ash Cement Pastes', CBI Research 2.81 (Swedish Cement and Concrete Research Institute, Stockholm, 1981).
10. Diamond, S., 'Minimal pozzolanic reaction in one year old fly ash pastes: an SEM evaluation', in Proceedings of 11th International Conference on Cement Microscopy, New Orleans, 1989 (International Cement Microscopy Association, Duncanville, TX) pp. 263–274.
11. Xu, A. and Sarkar, S. L., 'Gypsum activated fly ash hydration in cement pastes', *Cem. Concr. Res.* **21** (1991) 1137–1147.
12. Wendlandt, W. W., 'Thermal Analysis', 3rd Edn (Wiley, London, 1986).
13. Pope, M. I. and Judd, M. D., 'Differential Thermal Analysis' (Heyden, London, 1977).
14. Ramachandran, V. S., 'Estimation of $Ca(OH)_2$ and $Mg(OH)_2$ – implications in cement chemistry', *Israel J. Chem.* **22** (1982) 240–246.
15. Schwiete, H. E. and Ludwig, U., 'Crystal structures and properties of cement hydration products (hydrated calcium aluminates and ferrites)', in Proceedings of 5th International Symposium on the Chemistry of Cement, Tokyo, 1968, Vol. II (Cement Association of Japan, Tokyo) pp. 37–67.
16. Grandet, J. and Ollivier, J. P., 'Nouvelle méthode d'étude des interfaces ciment–granulats', Proceedings of 7th International Congress on the Chemistry of Cement, Paris, 1980, Vol. III (Editions Septima, Paris) pp. VII 85–89 (in French).
17. Larbi, J. A. and Bijen, J. M., 'Evolution of lime and microstructural development in fly ash–Portland cement specimens', *Mater. Res. Soc. Symp. Proc.* **178** (1990) 127–138.
18. *Idem.*, 'Orientation of calcium hydroxide at the Portland cement paste–aggregate interface in mortars in the presence of silica fume: a contribution', *Cem. Concr. Res.* **20** (1990) 461–470.
19. Grandet, J. and Ollivier, J. P., 'Orientation des hydrates au contact des granulats', in Proceedings of

7th International Congress on the Chemistry of Cement, Paris, 1980, Vol. III (Editions Septima, Paris) pp. VII 63–68 (in French).
20. Barnes, B. D., Diamond, S. and Dolch, W. L., 'The contact zone between Portland cement paste and glass "aggregate" surfaces', *Cem. Concr. Res.* **8** (1978) 233–243.
21. Massazza, F. and Costa, U., 'Bond: paste–aggregate, paste–reinforcement and paste–fibres', in Proceedings of 8th International Congress on the Chemistry of Cement, Rio de Janeiro, 1986, Vol. I (Finep Publications, Rio de Janeiro) pp. 158–180.
22. Buckley, H. E., 'Crystal Growth' (Wiley, London, 1951).
23. Taylor, H. F. W., 'Chemistry of cement hydration', in Proceedings of 8th International Congress on the Chemistry of Cement, Rio de Janeiro, 1986, Vol. I (Finep Publications, Rio de Janeiro) pp. 82–110.
24. Copeland, L. E. and Kantro, D. L., 'Hydration of Portland cement', in Proceedings of 5th International Symposium on the Chemistry of Cement, Tokyo, 1968, Vol. II (Cement Association of Japan, Tokyo) pp. 386–421.
25. Kondo, R. and Ueda, S., 'Kinetics and mechanisms of the hydration of cements', *ibid.* pp. 203–255.
26. Larbi, J. A. and Bijen, J. M., 'Effects of water-cement ratio, quantity and fineness of sand on the evolution of lime in set Portland cement systems', *Cem. Concr. Res.* **20** (1990) 783–794.
27. Berntsson, L., Chandra, S. and Kutti, T., 'Principles and factors influencing high-strength concrete production', *Concr. Internatl* **12**(12) (1990) 59–62.
28. Ahmed, S. J., Glasser, L. S. D. and Taylor, H. F. W., 'Crystal structures and reactions of C_4AH_{12} and derived basic salts', in Proceedings of 5th International Symposium on the Chemistry of Cement, Tokyo, 1968, Vol. II (Cement Association of Japan, Tokyo) pp. 118–127.

RESUME

Les effets des cendres volantes sur la microstructure des mortiers de ciment

Une étude microstructurale de mortiers préparés à partir de ciment à faible teneur en alcali et en C_3A ainsi que de cendres volantes de classe F (tous deux d'origine suédoise) a été menée en se servant du microscope électronique à balayage et de la technique d'analyse de rayons X à dispersion d'énergie. Les phases supplémentaires étaient étudiées par thermogravimétrie et analyse thermique différentielle.

Normalement, les critaux de CH croissent dans la zone de transition en sorte que leur axe est parallèle à la surface du granulat (ou le plan de clivage (0 0 1) perpendiculaire à la surface). En croissant le CH recouvre les cendres volantes, ce qui réduit la quantité de CH orienté à l'interface pâte–granulat. La diminution de CH, très importante après 28 jours, semble dépendre surtout de la réaction entre les cristaux de CH et la phase vitreuse des cendres volantes.

Au début de l'hydratation, l'addition de cendres volantes affaiblit la zone d'interface entre la pâte et le granulat en réduisant les points de contact. Le rapport eau–ciment local est aussi augmenté. Une fois que la réaction des cendres volantes commence, la situation s'améliore de façon significative. Afin d'augmenter la réactivité des cendres volantes, on a ajouté du gypse. Les résultats démontrent que, bien que le gypse puisse accélérer la réaction des cendres volantes, la formation de produits de réaction, ainsi que les avantages, dépendent de la quantité totale de gypse dans la pâte.